Journal of Computational Methods in Molecular Design, 2016, 6 (2):39-59

ISSN : 2231- 3176
CODEN (USA): JCMMDA

Vibrational, NMR and UV-Visible spectroscopic investigation, HOMO-LUMO and NLO studies on Bis(thiourea) Cadmium chloride (BTCC) Using quantum mechanical simulations

R. Durga[a], R. S. Sundararajan[b], S. Anand[a,*], C. Ramachandraraja[b] and S. Ramalingam[a]

[a] *Department of Physics, A.V.C. College, Mayiladuthurai, Tamilnadu, India.*
[b] *Department of Physics, Government Arts College, Kumbakonam, Tamilnadu, India.*
Corresponding E-mail: anandphy09@gmail.com

ABSTRACT

In the present research work, the FT-IR, FT-Raman spectra of the Bis(thiourea) Cadmium chloride (BTCC) were recorded. The observed fundamental frequencies in finger print and functional group regions were assigned according to their uniqueness region. The computational calculations were carried out by HF and DFT (B3LYP, CAM – B3LYP, B3PW91 and MPW1PW91) methods with 3-21 G(d, p) basis set and the corresponding results were tabulated. The present compound is an organo-metallic compound which is made up of covalent and coordination covalent bonds and the modified vibrational pattern of the complex molecule associated with ligand group was analyzed. Moreover, ^{13}C NMR and ^{1}H NMR were calculated by using the gauge independent atomic orbital (GIAO) method with B3LYP methods and the 6-311++G(d,p) basis set and their spectra were simulated and the chemical shifts linked to TMS were compared. A study on the electronic and optical properties; absorption wavelengths, excitation energy, dipole moment and frontier molecular orbital energies were carried out. The kubo gap of the present compound was calculated related to HOMO and LUMO energies which confirm the occurring of charge transformation between the base and ligand. Besides frontier molecular orbitals (FMO), molecular electrostatic potential (MEP) was performed. The NLO properties related to Polarizability and hyperpolarizability based on the finite-field approach were also discussed. A new semiorganic nonlinear optical crystal of Bis(thiourea) Cadmium chloride (BTCC) was grown successfully by slow evaporation technique using water as solvent. The lattice parameters of the grown crystal have been determined by X-ray diffraction studies. Vibrational spectrum is recorded to determine symmetries of molecular vibrations. The recording of Optical absorbance spectrum revealed that this crystal has good transparency in the visible region. The nonlinear nature of the present crystal has been confirmed by the SHG test. Vickers micro-hardness test has done on the crystal and this shows that the crystal has greater physical strength.

Key words: BTCC, NLO, Homo-Lumo, GIAO, Chemical shifts, FMO, MEP.

INTRODUCTION

The preparation of crystals by combining the high non linear optical activity of the organic molecules with the excellent physical properties of the inorganics (metal compound) has been found to be overpoweringly successful in the recent past [1]. Because, now a days, many industry needed such high efficiency crystals for many electric and electronic applications. Thiourea, which is otherwise centro-symmetric, yields excellent noncentro-symmetric materials and typifies this approach. Metal-organic compounds as NLO materials have attracted much more attention for their high NLO coefficients, stable physico-chemical properties and better mechanical intension.
Nonlinear optical (NLO) materials play an important role in nonlinear optics, optical communication, optical switching, optical disk data storage, laser fusion reactions, optical rectifications and in particular they have a great

impact on information technology and industrial applications [2-7]. The approach of combining the high nonlinear optical coefficient of the organic molecules with the excellent physical properties of the inorganics was found to be extremely successful in the recent past [8-12].

The thiourea molecule is an interesting inorganic matrix modifier due to its large dipole moment [13] and its ability to form an extensive network of hydrogen bonds [14]. The metal complexes of thiourea which have low UV cut off wavelengths, applicable for high power frequency conversion have received much attention. Ligands like thiourea form stable complexes through coordinated bonds by S and N donors which are adequate to combine with metal [15]. The centrosymmetric thiourea molecule, when combined with inorganic salt yields noncentrosymmetric complexes, which have the NLO properties [16] and also some of them found centrosymmetric in nature [17-19]. The thiourea is also used to accelerate and stereochemically alter organic transformations through predominantly double hydrogen-bonding interactions with the respective substrate(s) (non-covalent organocatalysis). Based on the intuitive approach to introduce the asymmetric conjugated organic molecules into an inorganic metal ion, several thiourea complexes were crystallized and their properties screened for their applications and Bis(thiourea) Cadmium Chloride (BTCC) [20] was identified as one of the promising candidates.

So, studies on the structures, physico-chemical and electro-optical properties of this organo-metal complex are very imperative to bring it out industrially. The literature survey reveals that, to the best of our knowledge, no intensive observation of spectroscopic [FT-IR and FT-Raman] and theoretical [HF/DFT] investigation has been reported so far. Therefore, the present investigation was undertaken to study the vibrational spectra, geometrical frame work review, inter and intra molecular interaction between HOMO and LUMO energy levels and first order hyperpolarizability of non linear optical (NLO) activity of the Bis(thiourea) Cadmium chloride.

MATERIALS AND METHODS

The compound BTCC is purchased from Sigma–Aldrich Chemicals, USA, which is of spectroscopic grade and hence used for recording the spectra as such without any further purification. The FT-IR spectrum of the compound is recorded in Bruker IFS 66V spectrometer in the range of 4000 – 100 cm^{-1}. The spectral resolution is ±2 cm^{-1}. The FT-Raman spectrum of AMS is also recorded in the same instrument with FRA 106 Raman module equipped with Nd:YAG laser source operating at 1.064 µm line widths with 200 mW power. The spectra are recorded in the range of 4000 – 100 cm^{-1} with scanning speed of 30 cm^{-1} min^{-1} of spectral width 2 cm^{-1}. The frequencies of all sharp bands are accurate to ±1 cm^{-1}. The absorption spectrum of BTCC was recorded using Varion Cary 5E UV-Vis-NIR spectrophotometer in the range 200 – 700 nm with high resolution. Single crystal XRD analysis was carried out using on Enraf Nonius CAD-4. X-ray diffractometer with M_0K_α (λ = 0.770 Å) radiation to identify the structure and presence of functional groups in BTCC qualitatively, estimate lattice parameter values. The sample was in a pellet form in KBr phase. The nonlinear property of BTCC crystals was confirmed from second harmonic generation test by using Nd:YAG laser beam. The physical strength of the crystal was measured by Vicker's microhardness test.

BTCC crystal was synthesized by dissolving AR grade thiourea and AR grade cadmium chloride in the molar ratio 2:1 in distilled water. The saturated solution of cadmium chloride is slowly added to the saturated solution of thiourea. This is stirred well to get a clear solution. The solution was purified by repeated filtration. The saturated solution was kept in a beaker covered with polythene paper. For slow evaporation, 6 or 7 holes are made in the polythene paper. Then, the solution is left undisturbed in a constant temperature bath (CTB) kept at a temperature of 35°C with an accuracy of ±0.1°C. As a result of slow evaporation, after 75 days colorless and transparent pure BTCC crystals were obtained as shown in Figure 1.

COMPUTATIONAL METHODS

Generally, the methodological investigation of vibrational spectroscopy along with quantum computational calculations is a potent tool for the thoughtful of fundamental vibrational behavior of

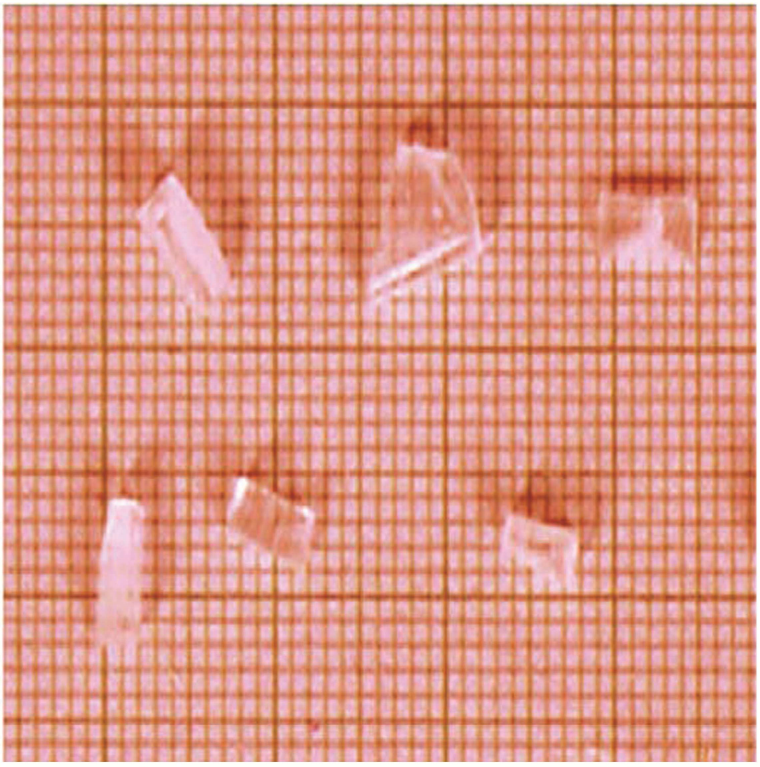

Figure 1: Photograph of (BTCC)
Bisthiourea Cadmium Chloride Crystals

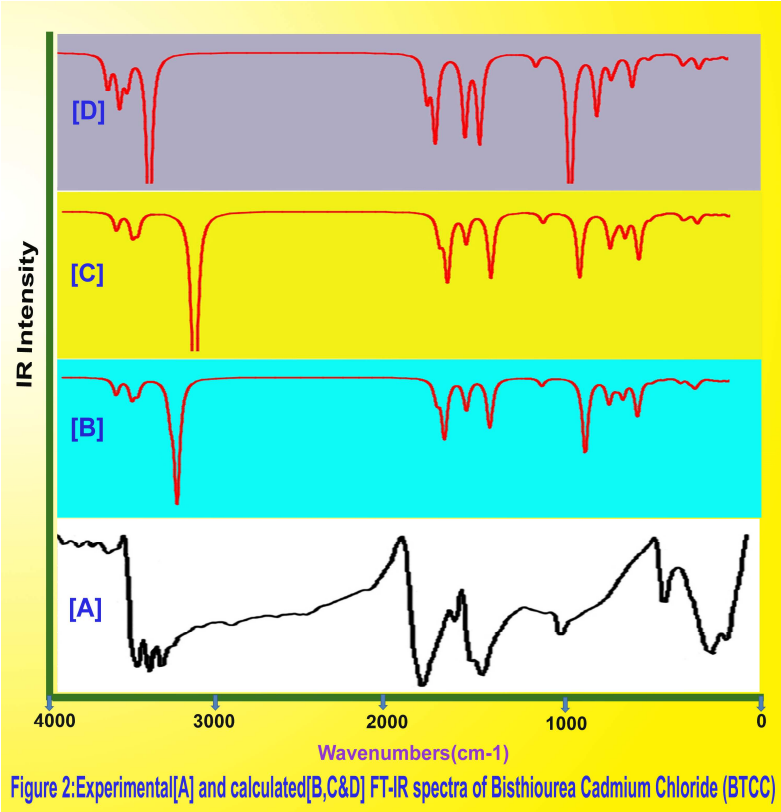

Figure 2:Experimental[A] and calculated[B,C&D] FT-IR spectra of Bisthiourea Cadmium Chloride (BTCC)

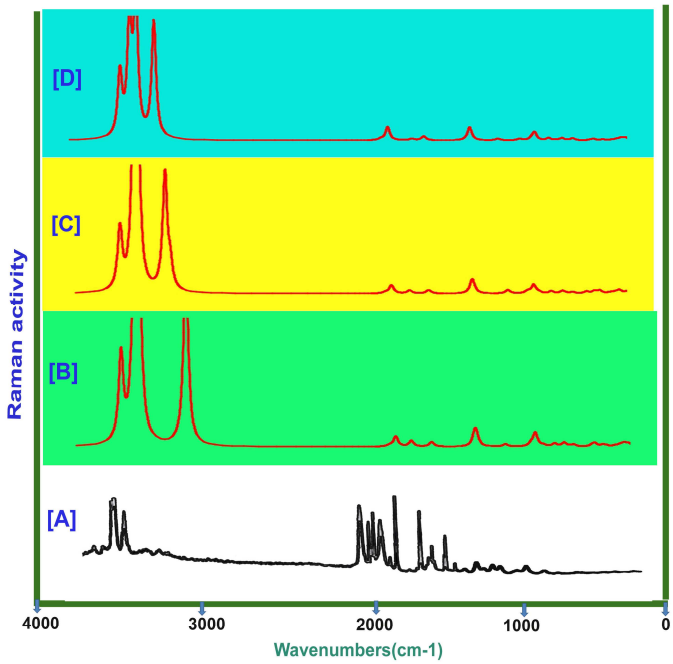

Figure 3:Experimental[A] and calculated[B,C&D] FT-Raman spectra of Bisthiourea Cadmium Chloride(BTCC)

a molecule. In the present work, the computational calculations were carried out by HF and DFT (B3LYP, CAM – B3LYP, B3PW91 and MPW1PW91) methods with 3-21 G (d, p) basis set. All these calculations were performed using GAUSSIAN 09W [21] program package on Pentium i3 processor in personal computer. In DFT methods; Becke's three parameter hybrids function combined with the Lee-Yang-Parr correlation function (B3LYP) [22-23], Becke's three parameter exact exchange-function (B3) [24] combined with gradient-corrected correlational functional of Lee, Yang and Parr (LYP) [25-26] and Perdew and Wang (PW91) [26-27] predict the best results for molecular geometry and vibrational frequencies for moderately larger molecules. The calculated frequencies are scaled down to yield the coherent with the observed frequencies. The scaling factors are 0.86, 0.87, 0.88, 0.94, 1.05, 1.18 and 1.26 for HF/3-21 G (d, p) method. For B3LYP/CAM - B3LYP/3-21 G (d, p) basis set, the scaling factors are 0.92, 0.94, 0.96, 1.28 and 1.32/0.92, 0.93, 0.94, 1.25 and 1.35. For B3PW91/3-21 G (d, p) basis set, the scaling factors are 0.92, 0.93, 0.94, 1.28 and 1.38. For MPW1PW91/3-21 G (d, p) level of basis set, the scaling factors such as 0.91, 0.92, 0.94, 1.26 and 1.35 are used. The observed (FT-IR and FT-Raman) and calculated vibrational frequencies and vibrational assignments are submitted in Table 1. Experimental and simulated spectra of IR and Raman are presented in the Figures 2 and 3, respectively.

The ^{1}H and ^{13}C NMR isotropic shielding are calculated with the GIAO method [28] using the optimized parameters obtained from B3LYP/6-311++G(d,p) method. ^{13}C isotropic magnetic shielding (IMS) of any X carbon atoms is made according to value ^{13}C IMS of TMS, $CS_X=IMS_{TMS}$. The ^{1}H and ^{13}C isotropic chemical shifts of TMS at B3LYP methods with 6-311++G(d,p) level using the IEFPCM method in DMSO, chloroform and CCl_4. The absolute chemical shift is found between isotropic peaks and the peaks of TMS [29].

The electronic properties; HOMO-LUMO energies, absorption wavelengths and oscillator strengths are calculated using B3LYP method of the time-dependent DFT (TD-DFT) [30-32], basing on the optimized structure in gas phase and solvent [DMSO, chloroform and CCl_4] mixed phase. Thermodynamic properties have been calculated from 100-1000ºC in gas phase using B3LYP/6-311++G(d,p) method. Moreover, the dipole moment, nonlinear optical (NLO) properties, linear polarizabilities and first hyperpolarizabilities and chemical hardness have also been studied.

RESULTS AND DISCUSSION

Molecular geometry

The molecular structure of BTCC is an orthorhombic crystal system and belongs to C_{2V} point group symmetry. The molecular structure is optimized by Berny's optimization algorithm using Gaussian 09 and Gauss view program and is shown in Figure 4. The comparative optimized structural parameters such as bond length, bond angle and dihedral angle are presented in Table 2. The present compound contains Cadmium metal atom, chloride atoms and four amino groups.

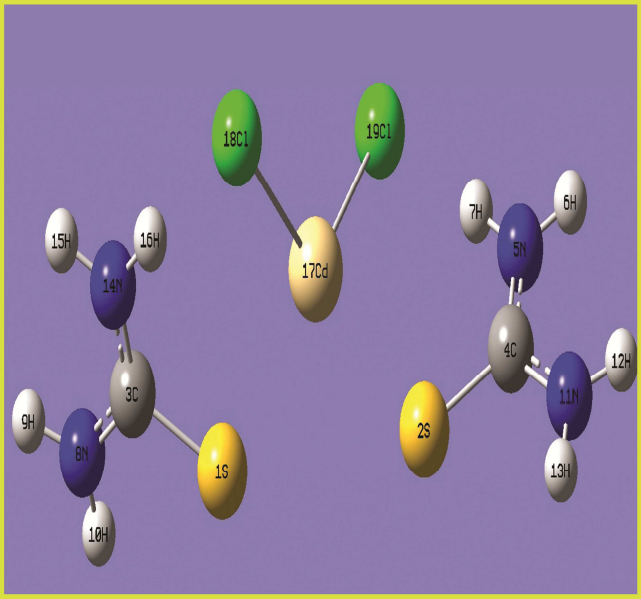

Figure 4: Molecular Structure of Bisthiourea Cadmium Chloride (BTCC)

The structure optimization and zero point vibrational energy of the compound in HF and DFT (B3LYP, CAM – B3LYP, B3PW91 and MPW1PW91) methods with 3-21 G (d, p) basis set are 87.41, 80.77, 82.08, 81.19 and 81.83 Kcal/Mol, respectively. The calculated energy of HF is greater than DFT method because the assumption of ground state energy in HF is greater than the true energy. Though, the molecular structure belongs to one plane, with respect to Cadmium chloride the thiourea on both sides are somewhat titled due to attraction between C*l* and H. Since the present compound is made up of metal atom and organic molecules, the entire atoms are connected by covalent and co-ordination covalent bonds. The Cadmium metal atom is connected with couple of thiourea by van der Walls bonds. Normally, the metal ions make dative bond with organic atoms to form organo-metallic compound due to which the considerable amount of energy is released and make a crystal very strong.

The experimental bond length of C-S and C-N are 1.720 and 1.340 Å whereas the calculated bond lengths are 1.771 and 1.339 Å respectively. Though, both the amino groups are coupled with carbon symmetrically, the bond distance of C-N is differed between them due to the attraction of H by C*l*. Normally, the double bond is to be there between C and S atoms, but one bond alone is there due to 2 lone pairs of electrons are transferred from ligand to metal (S to Cd). The calculated bond length of Cd-S is 2.744 Å which is long and strong van der Waals bond. The internuclear distance of N5 – H7 = N14 – H16 is 1.0084 Å and this value is greater than that of N5 – H6 = N14 – H15. This variation exists due to the attraction of C*l* and H atoms. Moreover, in this compound, both the amino groups are coupled with carbon atom in symmetrical manner. From the optimized parameters, it is inferred that, the organo-metallic compound is very strong due to the complex bonds.

Vibrational assignments

In order to obtain the spectroscopic signature of the BTCC, the computational calculations are carried out for frequency analysis. The molecule is identified with C_{2V} point group symmetry, consists of 19 atoms, so that it has 51 normal vibrational modes. On the basis of C_{2V} symmetry, the 51 fundamental vibrations of the molecule can be distributed as

$$\mathbf{\Gamma\ Vib = 19A_1 + 7A_2 + 11B_1 + 14B_2}$$

A_1 and B_2 irreducible representations correspond to stretching, ring deformation and in plane bending vibrations while A_2 and B_1 correspond to ring, torsion and out of plane bending vibrations. The harmonic vibrational frequencies (scaled and unscaled) calculated at HF and DFT (B3LYP, CAM – B3LYP, B3PW91 and MPW1PW91) levels using the triple split valence basis set along with the diffuse and polarization functions; 3-21 G (d, p) and observed FT-IR and FT-Raman frequencies for various modes of vibrations have been presented in Tables 1 and 3. Comparison of calculated frequencies with the experimental values reveal the over estimation of the calculated vibrational modes due to the neglect of a harmonicity and change of state of a real system.

Table 1: Observed and calculated vibrational frequencies of Bis(thiourea) Cadmium Chloride (BTCC) computed at HF & DFT (B3LYP, CAM – B3LYP, B3PW91 & MPW1PW91) with 3-21G (d, p) basis sets

S. No	Symmetry Species C_{2v}	Observed Frequency(cm^{-1})		Methods					Vibrational Assignments
				HF	B3LYP	CAM - B3LYP	B3PW91	MPW1PW91	
		FTIR	FT-Raman	3-21G (d, p)	3-21G (d, p)	3-21G (d, p)	3-21G (d, p)	3-21G (d, p)	
1	A_1	3360 s	3340 s	3369	3346	3375	3347	3358	**(N-H)** υ
2	A_1	3355 vs	3335 s	3330	3345	3337	3338	3357	**(N-H)** υ
3	A_1	3330 vs	-	3325	3332	3327	3323	3327	**(N-H)** υ
4	A_1	3310 s	3310 m	3306	3305	3309	3309	3309	**(N-H)** υ
5	A_1	3305 s	-	3302	3299	3300	3295	3297	**(N-H)** υ
6	A_1	3300 s	-	3301	3298	3282	3294	3295	**(N-H)** υ
7	A_1	3260 s	3240 w	3259	3247	3262	3236	3258	**(N-H)** υ
8	A_1	3255 vs	3235 w	3252	3243	3261	3234	3254	**(N-H)** υ
9	A_1	1620 s	-	1619	1615	1616	1618	1615	**(N-H)** δ
10	A_1	1610 m	1600 m	1618	1614	1614	1598	1608	**(N-H)** δ
11	A_1	1600 s	1590 m	1592	1589	1586	1590	1600	**(N-H)** δ
12	B_2	1575 s	-	1573	1572	1585	1573	1574	**(N-H)** δ
13	B_2	1550 w	1530 vs	1546	1562	1547	1549	1545	**(N-H)** δ
14	A_1	1500 m	-	1496	1497	1498	1484	1496	**(N-H)** δ
15	A_1	1480 s	-	1479	1470	1469	1466	1477	**(N-H)** δ
16	A_1	1460 w	1440 s	1459	1463	1451	1451	1459	**(N-H)** δ
17	A_1	1430 s	-	1423	1425	1422	1424	1426	**(N-H)** δ
18	A_1	1390 s	-	1386	1381	1387	1378	1379	**(C-N)** υ
19	B_2	1320 s	1300 s	1318	1336	1309	1316	1314	**(C-N)** υ
20	B_2	1270 s	1250 m	1269	1281	1263	1260	1269	**(C-N)** υ
21	B_2	1250 m	1230 m	1246	1244	1248	1246	1248	**(C-S)** υ
22	B_2	1220 w	-	1214	1214	1246	1243	1245	**(C-S)** υ
23	B_2	1200 s	-	1193	1195	1195	1195	1197	**(C-N)** υ
24	B_2	990 m	980 w	987	986	1007	993	984	**(N-H)** γ
25	B_1	870 m	-	867	866	863	868	868	**(N-H)** γ
26	B_1	730 w	710 w	734	722	724	728	727	**(N-H)** γ
27	A_2	700 w	-	710	696	698	693	705	**(N-H) γ**
28	A_2	660 w	-	666	658	658	655	640	**(N-H) γ**
29	A_2	610 w	-	602	601	607	605	606	**(N-H) γ**
30	A_2	570 w	-	564	566	557	568	553	**(N-H) γ**
31	B_2	520 w	-	533	513	518	519	521	**(N-H) γ**
32	B_2	500 m	-	501	484	502	497	482	**(Cd-C*l*)** υ
33	A_1	480 m	470 w	499	462	477	475	477	**(Cd-C*l*)** υ
34	A_1	430 w	-	428	444	426	423	433	**(Cd-S)** υ
35	A_1	410 m	-	420	394	413	410	413	**(Cd-S)** υ
36	B_2	400 m	380 w	399	393	411	407	387	**(C-N)** δ
37	B_2	390 w	370 w	361	388	392	393	356	**(C-N)** δ
38	A_2	370 w	-	328	312	363	360	353	**(C-S)** δ
39	A_2	320 m	300 w	241	274	279	278	275	**(C-S)** δ
40	A_2	295 m	280 w	233	262	275	274	271	**(C-N) γ**
41	B_2	275 w	-	205	242	248	245	243	**(C-N) γ**
42	B_2	230 w	220 vw	192	176	245	242	240	**(C-S) γ**
43	B_1	205 w	190 vw	147	143	159	158	156	**(C-S) γ**
44	B_1	180 w	-	110	114	116	114	113	**(Cd-C*l*)** δ
45	B_1	175 w	-	100	106	112	111	109	**(Cd-C*l*)** δ
46	B_1	150 w	-	95	95	101	102	100	**(Cd-S)** δ
47	B_1	140 w	-	78	80	90	89	88	**(Cd-S)** δ
48	B_1	130 w	110 vw	70	77	79	80	78	**(Cd-C*l*) γ**
49	B_1	120 w	100 vw	49	63	58	55	55	**(Cd-C*l*) γ**
50	B_1	110 w	-	18	20	16	17	19	**(Cd-S) γ**
51	B_1	95 w	-	10	7	14	14	14	**(Cd-S) γ**

s – Strong; m- Medium; w – weak; as- Asymmetric; s – symmetric; υ – stretching; α –deformation, δ - In plane bending; γ-out plane bending; τ – Twisting:

Table 2: Optimized geometrical parameters for Bis(thiourea) Cadmium Chloride (BTCC) computed at HF & DFT (B3LYP, CAM – B3LYP, B3PW91 & MPW1PW91) with 3-21G (d, p) basis sets

Geometrical Parameters	Methods				
	HF	B3LYP	CAM – B3LYP	B3PW91	MPW1PW91
	3-21G (d-p)	3-21G (d-p)	3-21G (d-p)	3-21G (d-p)	3-21G (d-p)
Bond length(Å)					
(S1-C3)	1.7841	1.7835	1.7716	1.7719	1.7692
(S1-Cd17)	2.744	2.6811	2.6571	2.6726	2.6647
(S2-C4)	1.7841	1.7838	1.7711	1.7714	1.7684
(S2-Cd17)	2.7442	2.6816	2.6547	2.6707	2.663
(C3-N8)	1.3271	1.3427	1.339	1.3441	1.3411
(C3-N14)	1.311	1.3311	1.3214	1.3264	1.3237
(C4-N5)	1.311	1.3312	1.3211	1.3259	1.3232
(C4-S1)	1.3272	1.3426	1.3393	1.3446	1.3417
(N5-H6)	1.0004	1.0176	1.016	1.0165	1.0149
(N5-H7)	1.0084	1.0299	1.0326	1.0361	1.0338
(N8-H9)	0.999	1.016	1.0139	1.0145	1.0129
(N8-H10)	0.9979	1.0138	1.0127	1.0131	1.0116
(N11-H12)	0.999	1.016	1.0139	1.0143	1.0128
(N11-H13)	0.9979	1.0138	1.0127	1.0131	1.0116
(N14-H15)	1.0004	1.0176	1.016	1.0165	1.0149
(N14-H16)	1.0084	1.0299	1.0326	1.0361	1.0339
(Cd17-C*l*18)	2.5444	2.4867	2.5142	2.5258	2.5206
(Cd17- C*l*19)	2.5443	2.6181	2.5155	2.5277	2.5225
Bond angle(˚)					
(C3-S1-Cd17)	111.7343	98.751	107.6521	106.8879	106.7085
(C4-S2-Cd17)	111.6752	98.3964	109.077	109.1068	109.133
(S1-C3-N8)	116.7721	117.3591	116.5078	116.5009	116.5252
(S1-C3-N14)	123.8584	122.8035	123.8226	123.6831	123.667
(N8-C3-N14)	119.3653	119.8253	119.663	119.8083	119.7999
(S2-C4-N5)	123.8508	122.7653	124.0413	124.0012	124.0181
(S2-C4-N11)	116.7791	117.3873	116.3291	116.2383	116.2416
(N5-C4-N11)	119.3657	119.8356	119.6252	119.7565	119.7363
(C4-N5-H6)	121.6939	121.7047	121.4472	121.5636	121.5346
(C4-N5-H7)	121.7535	121.1931	121.6652	121.5031	121.5533
(H6-N5-H7)	116.5461	116.9298	116.878	116.9193	116.898
(C3-N8-H9)	122.5344	122.6683	122.5511	122.6272	122.607
(C3-N8-H10)	119.2225	118.6566	118.7002	118.6119	118.6312
(H9-N8-H10)	118.243	118.6674	118.7486	118.7582	118.7597
(C4-N11-H12)	122.5342	122.6705	122.5366	122.6044	122.5802
(C4-N11-H13)	119.2219	118.6463	118.7252	118.6459	118.6668
(H12-N11-H13)	118.2438	118.6731	118.7378	118.7478	118.7513
(C3-N14-H15)	121.6914	121.6984	121.5005	121.64	121.6194
(C3-N14-H16)	121.76	121.2118	121.5355	121.3062	121.3434
(H15-N14-H16)	116.5425	116.9318	116.9477	117.0264	117.0107
(S1-Cd17-S2)	99.8947	110.4051	102.0841	101.6401	101.4124
(S1-Cd17-C*l*18)	101.1015	115.424	102.3707	102.012	101.9338
(S1-Cd17-C*l*19)	114.4109	100.4137	113.6616	113.6059	113.7267
(S2-Cd17-C*l*18)	114.3955	115.0124	115.0004	114.9624	115.1077
(S2-Cd17-C*l*19)	101.0681	100.3118	103.1216	103.2229	103.2265
(C*l*18-Cd17-C*l*19)	123.8774	113.3297	119.5763	120.1942	120.198
Dihedral angles(˚)					
(Cd17-S1-C3-N8)	163.4172	-141.7415	158.2812	156.9218	156.2035
(Cd17-S1-C3-N14)	-17.3348	39.5289	-22.6627	-24.0899	-24.828
(C3-S1-Cd17-S2)	138.8836	-160.7774	150.8795	153.1151	153.937
(C3-S1-Cd17-C*l*18)	21.4003	66.6655	31.5763	34.1444	34.9176
(C3-S1-Cd17-C*l*19)	-114.0684	-55.5558	-98.7994	-96.7095	-95.9611
(Cd17-S2-C4-N5)	-17.6456	-40.0168	-17.3635	-16.1248	-16.2676
(Cd17-S2-C4-N11)	163.1197	141.2395	163.404	164.6046	164.4647
(C4-S2-Cd17-S1)	139.2774	161.5576	142.3248	140.5789	140.5758
(C4-S2-Cd17-C*l*18)	-113.6415	-65.675	-107.7024	-110.1356	-110.3037
(C4-S2-Cd17-C*l*19)	21.7876	56.2676	24.2036	22.649	22.5985
(S1-C3-N8-H9)	178.4403	-175.7713	176.7876	175.8268	175.9245
(S1-C3-N8-H10)	-1.5233	5.2546	-3.0402	-3.5703	-3.5413
(N14-C3-N8-H9)	-0.8431	2.9978	-2.31	-3.203	-3.0862
(N14-C3-N8-H10)	179.1933	-175.9762	177.8622	177.4	177.448
(S1-C3-N14-H15)	179.593	-174.9237	178.2471	177.5022	177.6085
(S1-C3-N14-H16)	0.5187	0.3674	-0.2391	-0.5373	-0.4629
(N8-C3-N14-H15)	-1.1774	6.3769	-2.725	-3.5413	-3.455
(N8-C3-N14-H16)	179.7483	-178.332	178.7889	178.4192	178.4735

(S2-C4-N5-H6)	179.5521	174.7187	178.5489	178.2214	178.2961
(S2-C4-N5-H7)	0.5102	-0.3622	-0.2887	-0.3809	-0.2988
(N11-C4-N5-H6)	-1.2319	-6.5672	-2.2425	-2.5322	-2.4603
(N11-C4-N5-H7)	179.7262	178.3518	178.9199	178.8654	178.9447
(S2-C4-N11-H12)	178.3594	175.7805	177.3092	176.9165	176.9981
(S2-C4-N11-H13)	-1.5842	-5.3897	-2.4687	-2.5776	-2.5264
(N5-C4-N11-H12)	-0.9113	-3.0017	-1.9591	-2.3869	-2.3028
(N5-C4-N11-H13)	179.1451	175.8282	178.263	178.1189	178.1727

Table 3: Calculated unscaled frequencies of Bis (thiourea) Cadmium Chloride (BTCC) computed at HF & DFT (B3LYP, B3PW91, CAM - B3LYP & MPW1PW91) with 3-21G (d, p) basis sets

S. No	Observed frequency	Calculated frequency				
		HF	B3LYP	B3PW91	CAM - B3LYP	MPW1PW91
		3-21G	3-21G	3-21G	3-21G	3-21G
1	3360	3873	3637	3670	3669	3691
2	3355	3873	3636	3669	3668	3690
3	3330	3800	3545	3574	3578	3597
4	3310	3800	3443	3574	3578	3597
5	3305	3753	3510	3544	3549	3565
6	3300	3752	3509	3542	3549	3563
7	3260	3614	3314	3204	3262	3233
8	3255	3614	3276	3202	3261	3232
9	1620	1883	1737	1740	1757	1751
10	1610	1882	1736	1737	1755	1748
11	1600	1830	1691	1692	1706	1703
12	1575	1830	1691	1692	1705	1702
13	1550	1646	1562	1581	1595	1593
14	1500	1645	1560	1579	1594	1592
15	1480	1557	1428	1437	1455	1449
16	1460	1553	1421	1432	1451	1445
17	1430	1206	1114	1122	1138	1132
18	1390	1206	1114	1121	1137	1131
19	1320	1199	1104	1106	1119	1114
20	1270	1198	1104	1106	1118	1114
21	1250	989	858	903	925	911
22	1220	987	855	901	923	909
23	1200	823	716	720	747	730
24	990	823	715	720	746	729
25	870	735	672	689	691	695
26	730	734	669	687	690	693
27	700	710	633	630	659	641
28	660	709	633	630	658	640
29	610	602	547	550	557	556
30	570	601	545	547	557	553
31	520	533	467	481	485	484
32	500	533	466	478	483	482
33	480	499	445	432	459	442
34	430	498	444	423	454	433
35	410	420	394	410	413	413
36	400	420	393	407	411	410
37	390	287	294	285	291	287
38	370	261	237	261	269	264
39	320	192	208	202	207	204
40	295	185	199	199	204	201
41	275	163	184	178	184	180
42	230	163	134	176	182	178
43	205	117	109	115	118	116
44	180	88	87	83	86	84
45	175	80	81	81	83	81
46	150	76	72	74	75	74
47	140	62	61	65	67	65
48	130	56	59	58	59	58
49	120	39	48	40	43	41
50	110	14	15	13	12	14
51	95	8	5	10	10	10

Amino group vibrations

The molecule thiourea consists of couple of NH_2 groups on both sides; there is a possibility of eight N-H stretching vibrations. Normally, aliphatic primary amines are characterized by strong absorption in the region of 3450 – 3100 cm^{-1} due to the asymmetric and symmetric NH_2^+ stretching. Specifically, the symmetric N–H stretching vibrations

occur in the region 3100 – 3300 cm^{-1} [33]. The asymmetric N-H_2 stretching vibration appeared from 3300 – 3500 cm^{-1} and the symmetric NH_2 stretching is observed in the range 3350 – 3420 cm^{-1} [34]. Also the NH_2^+ asymmetric and symmetric deformation wave numbers are expected to fall in the regions 1660–1610 cm^{-1} and 1550–1485 cm^{-1}, respectively [35-36]. In this present case, the N-H stretching frequencies are observed at 3360, 3355, 3330, 3310, 3305, 3300, 3260 and 3255 cm^{-1}. The first three bands and second five bands are assigned to asymmetric and symmetric vibrations respectively. In addition to that, last two vibrational bands are found to be moved down from the expected region. This is mainly due to the presence of sulfur with chain. The N-H in plane bending vibrations (scissoring) are usually observed in the region 1610-1630 cm^{-1}, rocking vibrations are assigned in the range 1100-1200 cm^{-1} and the out-of-plane bending (wagging and twisting) vibrations are normally identified under 1150-900 cm^{-1} [37-39]. The in- plane deformation vibrations for the present compound are observed at 1620, 1610, 1600, 1575, 1550, 1500, 1480, 1460 and 1430 cm^{-1}. The first two bands are moved upto the higher region and it is cleared that, these vibrations are favoured. The out-of-plane bending vibrations are set up at 990, 870, 730, 700, 660, 610, 570 and 520 cm^{-1}. Normally, whenever the metal atom coupled with the organic molecules, the normal vibrational modes of the same are suppressed much. The entire out of plane bending vibrations are found out of the expected region. This view clearly shows that the N-H out-of-plane vibrations are hindering by other vibrations. From the N-H vibrations, it is observed that, the entire out-of-plane vibrational modes are affected by other substitutions in the chain.

C-N Vibrations

The C-N stretching frequency is rather difficult to task since there are problems in identifying these frequencies from other vibrations [40]. Silverstein [41] assigned C-N stretching vibrations in the region 1386 – 1266 cm^{-1} for aromatic amines. In this present work, the C-N Stretching is observed at 1390, 1320, 1270 and 1200 cm^{-1} which is making disagreement with the literature [42] due to the loading of sulfur and metal atoms with the molecule. The C-NH_2 in-plane and out-of-plane bending vibrations are appeared at 400 & 390 and 295 & 275 cm^{-1} respectively. These two vibrations are affected much by other vibrations which make disagreement with literature values [43-44].

C-S Vibrations

The thio-cyanate ion may act as an ambidentate ligand, i.e. bonding may occur either through the nitrogen or the sulphur atom. The bonding mode may easily be distinguished by examining the band due to the C-S stretching vibration which occurs at 730-690cm^{-1} [45-47]. In this present case, the C-S stretching vibrations are identified at 1250 cm^{-1} (medium intensity) and 1220 cm^{-1} (weak intensity) in IR spectrum. The observed bands are in line with the expected range and literature [48]. Generally, The C-S in-plane bending vibrations are observed in the region from 440-410 cm^{-1}[48]. In this metal organic compound, the in-plane bending vibrations are found at 370 & 320 cm^{-1} and the out-of-plane bending vibrations at 230 & 205 cm^{-1}. These vibrational bands are pulled down to the lower region of the expected range due to the Cd ion.

Cd-Cl and Cd-S Vibrations

The present molecule is a metal-organic crystal compound which has Cd metal ion coupled with couple of chlorine atoms by forming coordinate covalent bond. Generally, in Cadmium metal complex, the Cd-C*l* stretching is very significant and is observed in the region 525-220 cm^{-1} [49]. In this compound, the coordinate covalent bond stretching vibrations are identified at 500 and 480 cm^{-1}. The Cd-C*l* in-plane and out-of-plane bending vibrational peaks are appeared at 180 & 175 cm^{-1} and 130 & 120 cm^{-1} respectively. From the Cd-C*l* vibrations, it is inferred that, these vibrations have not affected much. This view clearly shows that, the metal-organic internuclear distance is made up of coordinate covalent bond and usually these vibrations will not be affected in order to emphasize its property.

In the present molecule, the organic compound; bisthiourea is directly connected through sulfur atom with metal chloride by forming coordinate covalent bond as S-Cd-S. Usually the Cd-S vibrations are pushed by organic vibrations due to the large force constants and strong covalent bonds. The Cd-S bond is made up of coordinate covalent bond which is very weak bond, its vibrations fallback to the Cd-C*l* vibrations. In this present case, the Cd-S stretching vibrations are observed at 430 and 410 cm^{-1}. The corresponding in-plane and out-of-plane bending vibrations are found at 150 & 140 cm^{-1} and 110 & 95 cm^{-1} respectively. The entire vibrations of Cd-S are observed in the lower range of the IR spectrum which shows the weak attraction of the bond between the metal and organic compound. Though the bond is weak, the crystal and chemical properties of the present compound are well. So, the crystal compound can be used for electric and electronic applications.

X – RAY DIFFRACTION ANALYSIS

Single Crystal XRD studies

The lattice dimensions and the crystal system have been determined from the single X-ray diffraction analysis (Model: ENRAFNONIUS CAD4). The determined unit cell parameters and the observed crystal system are reported

in the Table 4. The data reveals the fact that BTCC crystals posses bigger volume when compared with bisthiourea. This may be due to high atomic radius of cadmium chloride when compared with bisthiourea. The studies revealed that the crystal belongs to orthorhombic system.

Table 4: Single crystal XRD results of Bis(thiourea) Cadmium Chloride (BTCC)

Sl. No.	Crystal name	Axial lengths of unit cell (a, b and c)	Inter axial angles (α, β and γ)	Volume (Å^3)	Crystal system
1	Thiourea	a = 7.655 Å b = 8.537 Å c = 5.520 Å	α = 90° β = 90° γ = 90°	360.7	Orthorhombic
2	BTCC	a = 5.804 Å b = 6.463 Å c = 13.099 Å	α = 90° β = 90° γ = 90°	491.3	

Powder XRD studies

Powder XRD analysis of the grown BTCC crystals have been carried out using Rich Siefert diffractometer with Cu Kα λ = 1.5406 A° radiation on crushed powder of BTCC crystals. The recorded powder X-ray patterns are shown in Figure 5. The differences in amplitude of the peak can be attributed to the difference in grain size and orientation of the powdered grains of the experimental crystals. The observed diffraction is indexed by Rietveld index software package. The lattice parameters calculated by Reitveld software package are tabulated in Table 5. The data obtained by powder X-ray diffraction are in good agreement with the single crystal XRD data.

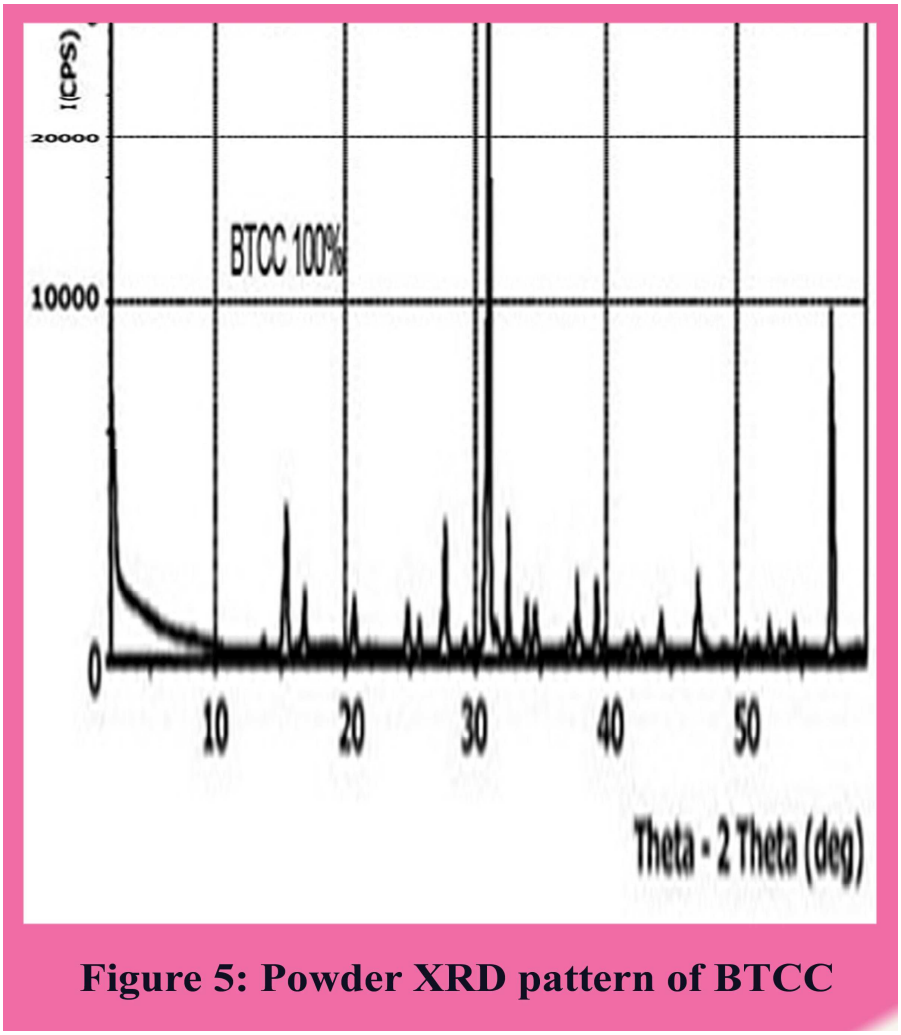

Figure 5: Powder XRD pattern of BTCC

Table 5: Powder XRD results of Bis(thiourea) Cadmium Chloride (BTCC)

Sl. No.	Crystal name	Observed a, b & c values by single XRD analysis	Calculated a, b & c values by powder XRD analysis	Observed volume by single XRD analysis (Å^3)	Calculated volume by powder XRD analysis (Å^3)
1	BTCC	a = 5.804 Å b = 6.463 Å c = 13.099 Å	a = 5.794 Å b = 6.461 Å c = 13.139 Å	491.3	491.91

NMR assessment

NMR spectroscopy technique is throwing new light on organic structure elucidation of much difficult complex molecules. The combined use of experimental and computational tools offers a powerful gadget to interpret and predict the structure of bulky molecules. The optimized structure of BTCC is used to calculate the NMR spectra at B3LYP method with 6-311++G(d,p) level using the GIAO method and the chemical shifts of the compound are reported in ppm relative to TMS for ^{1}H and ^{13}C NMR spectra which are presented in Table 6. The corresponding spectra are shown in Figure 6.

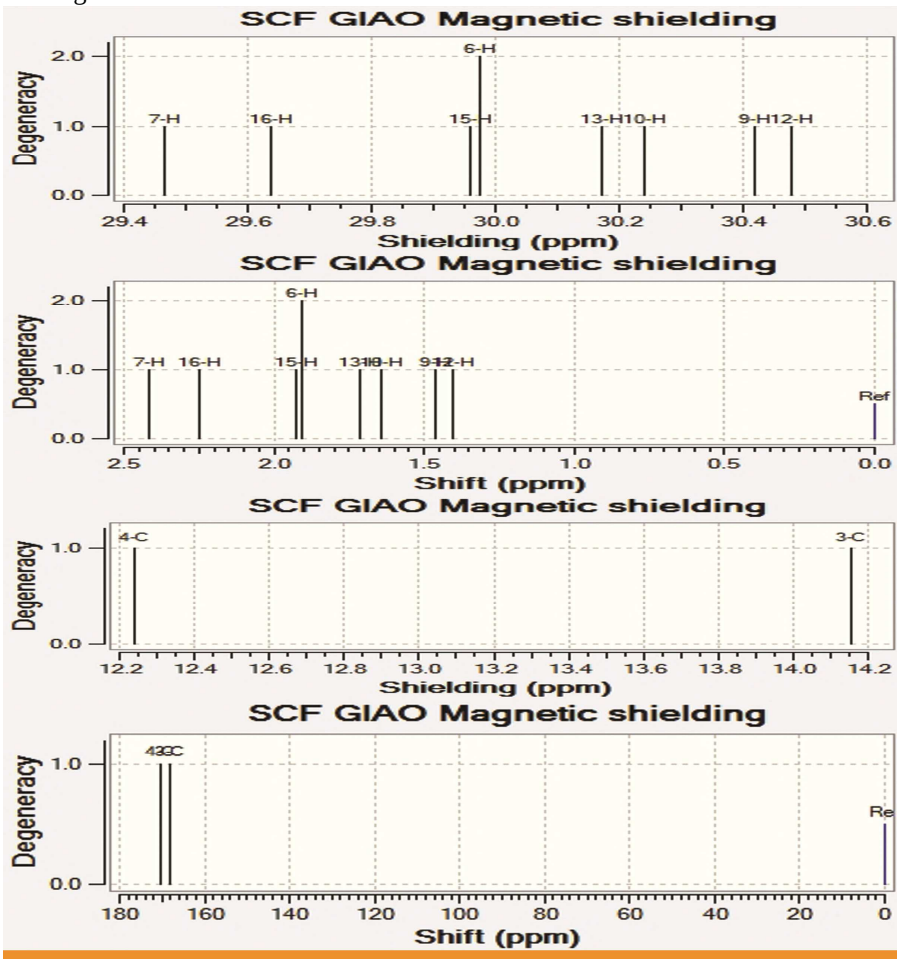

Figure 6: Simulated 13C & 1H NMR spectra of BTCC

Normally, the range of ^{13}C NMR chemical shifts for aromatic derivatives is greater than 100 ppm and the accuracy ensure that the reliable interpretation of spectroscopic parameters. In the present work, the metello organic compound has been taken for the study in which the molecule contains two carbons along with two amine group. The ^{13}C NMR chemical shift of such two carbons is greater than 100 ppm, as in the expected regions.

Table 6: Calculated ^{1}H and ^{13}C NMR chemical shifts (ppm) of Bis(thiourea) Cadmium Chloride (BTCC)

Atom position	B3LYP/6-311+G (d,p) (ppm)	TMS B3LYP/6-311+G (2d,p) GIAO (ppm)	Shift (ppm)	B3LYP/6-311+G (d,p) (ppm)	TMS B3LYP/6-311+G (2d,p) GIAO (ppm)	Shift (ppm)	B3LYP/6-311+G (d,p) (ppm)	TMS B3LYP/6-311+G (2d,p) GIAO (ppm)	Shift (ppm)	B3LYP/6-311+G (d,p) (ppm)	TMS B3LYP/6-311+G (2d,p) GIAO (ppm)	Shift (ppm)
	Gas			DMSO			Chloroform			CCl4		
C3	14.15	168.30	154.15	5.47	176.99	171.52	7.48	174.98	167.50	9.77	172.69	162.92
C4	12.24	170.22	157.98	4.31	178.15	173.84	6.22	176.23	170.01	8.35	174.11	165.76
H6	29.97	1.90	28.07	29.17	2.70	26.47	29.37	2.51	26.86	29.58	2.29	27.29
H7	29.46	2.41	27.05	29.35	2.52	26.83	29.37	2.51	26.86	29.40	2.47	26.93
H9	30.41	1.46	28.95	29.44	2.43	27.01	29.69	2.19	24.50	29.96	1.91	28.05
H10	30.24	1.64	28.60	29.64	2.23	27.41	29.79	2.09	27.70	29.95	1.92	28.03
H12	30.47	1.40	29.07	29.44	2.43	27.01	29.72	2.16	27.56	30.00	1.87	28.13
H13	30.17	1.71	28.46	29.61	2.26	24.35	29.74	2.14	27.60	29.89	1.99	27.90
H15	29.95	1.92	28.03	29.71	2.70	27.01	29.37	2.50	26.87	29.59	2.29	27.30
H16	29.63	2.24	27.39	26.36	2.52	23.84	29.40	2.47	26.93	29.59	2.41	27.18

In the case of BTCC, the chemical shift of C3 and C4 are 154.15 and 157.98 ppm respectively. The chemical shift is more or less same for C3 and C4 since both the carbons having similar groups. The chemical shift of both carbons is very high; it is also due to the migration of double bond from C-S to C-N. The chemical shift of H6, H7, H9, H10, H12, H13, H15 and H16 are 28.07, 27.05, 28.95, 28.60, 29.07, 28.46, 28.03 and 27.39 ppm respectively. From the result of shift of Hydrogen atom, it is observed that, the chemical shift of H12 is higher than rest of other hydrogen atoms in the chain. This is purely due to the extended influence on hydrogen atom by nearby chlorine atoms. From the entire chemical shift of the molecules it can be inferred that, the chemical property of the metal is directly mingled with organic molecules and this is the main cause for the present metal complex molecule having new chemical property.

Electronic properties (Frontier Molecular studies)

The electronic reconfiguration and electronic excitations in frontier molecular orbitals are very much useful for studying the electric and optical properties of the organic molecules. The stabilization of the bonding and destabilization of the antibonding of molecular orbital can be made by the overlapping of molecular orbitals. The stabilization of the bonding molecular orbital and destabilization of the antibonding molecular orbital can increase, when the overlap of two orbitals increases [50].

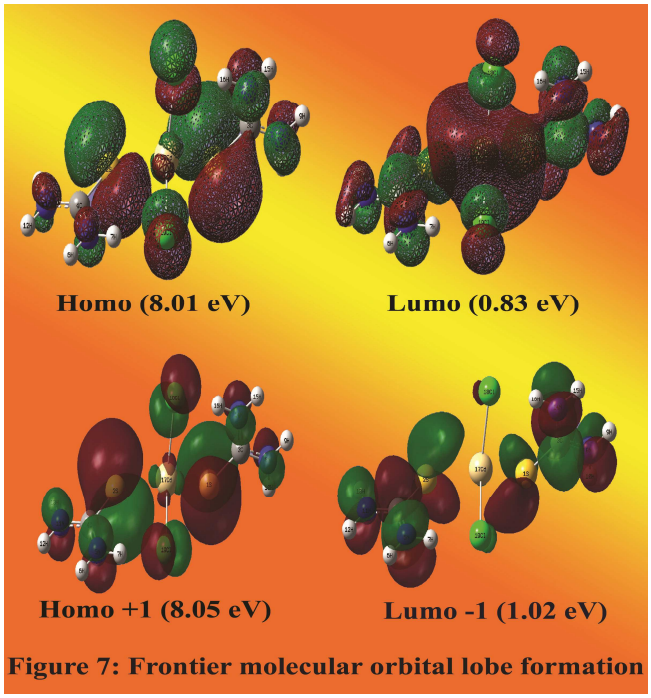

Figure 7: Frontier molecular orbital lobe formation

Table 7: Frontier molecular orbitals with energy levels of Bis(thiourea) Cadmium Chloride (BTCC)

Energy levels	Energy in eV
H+8	9.18
H+7	8.94
H+6	8.86
H+5	8.62
H+4	8.42
H+3	8.26
H+2	8.24
H+1	8.05
H	8.01
L	0.83
L-1	1.02
L-2	1.24
L-3	2.03
L-4	2.22
L-5	2.53
L-6	3.07
L-7	3.11
L-8	3.30
L-9	3.61
L-10	3.73

In molecular interaction, there are two important orbitals that interact with each other. One is the highest energy occupied molecular orbital called HOMO which represents the ability to donate an electron. The other one is the lowest energy unoccupied molecular orbital called LUMO which acts as an electron acceptor. These orbitals are also called the frontier orbitals. The interaction between them is much stable and is called filled empty interaction. When the two same sign orbitals overlap to form a molecular orbital, the electron density will occupy at the region between two nuclei. The molecular orbital resulting from in-phase interaction is defined as the bonding orbital which has lower energy than the original atomic orbital. The out-of-phase interaction forms the antibonding molecular orbital with the higher energy than the initial atomic orbital.

The 3D plots of the frontier orbitals, HOMO and LUMO for the present molecule are in gas, shown in Figure 7. According to such Figure, the HOMO is mainly localized over the Cadmium, C*l*, N atoms and C-S group in which there are two sigma bond interaction taking place over the C-S of thiourea and one delta bond interaction over Cadmium chloride. The N and C*l* atoms of the molecule are connected by S orbital lobes. However, LUMO is characterized by a charge distribution connects the Cadmium-chloride atoms and C-S bonds in which there are two sigma and one delta bond interactions taking place. From this observation, it is clear that, the in-phase and out-of-phase interactions are present in HOMO and LUMO respectively. The HOMO→LUMO transition implies an electron density transferred among Cadmium chloride and thiourea separately. The HOMO and LUMO energy are 8.01 eV and 0.83 eV in gas phase respectively (Table 7). Energy difference between HOMO and LUMO orbitals is called as energy gap (kubo gap) that is an important feature for the stability of structures.

Optical properties (HOMO-LUMO studies)

The UV and visible spectroscopy is used to detect the presence of chromophores in the molecule whether the compound has NLO properties or not. The calculations of the electronic structure of BTCC are optimized in singlet state. The low energy electronic excited states of the molecule are calculated at the B3LYP/6-311++G(d,p) level using the TD-DFT approach on the previously optimized ground-state geometry of the molecule. The calculations are performed in gas phase and with the solvent of DMSO, chloroform and CCl_4. The calculated excitation energies, oscillator strength (*f*), wavelength (λ) and spectral assignments are given in Table 8. The major contributions of the transitions are designated with the aid of SWizard program [51].

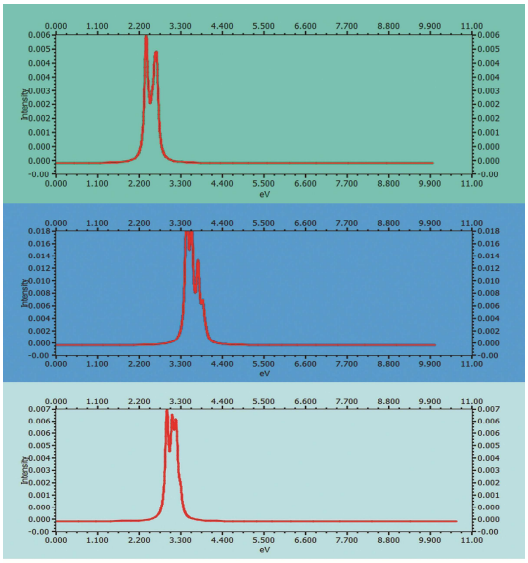

Figure 8: Simulated UV - Visible spectra of BTCC

Table 8: Theoretical electronic absorption spectra of Bis(thiourea) Cadmium Chloride (BTCC) (absorption wavelength λ (nm), excitation energies E (eV) and oscillator strengths (*f*)) using TD-DFT/B3LYP/6-311++G(d, p) method
H: HOMO; L: LUMO

λ (nm)	E (eV)	(*f*)	Major contribution	Assignment	Region	Bands
Gas						
518.69	2.3903	0.0055	H→L (90%)	n→σ*	Visible	R-band (German, radikalartig)
505.48	2.4528	0.0008	H→L (88%)	n→σ*	Visible	
487.50	2.5433	0.0013	H→L-1 (84%)	n→σ*	Visible	
474.04	2.6155	0.0026	H+1→L (85%)	n→σ*	Visible	
470.83	2.6333	0.0002	H→L-1 (91%)	n→π*	Visible	
463.68	2.6739	0.0035	H+1→L (86%)	n→π*	Visible	
DMSO						
358.40	3.4594	0.0125	H→L (92%)	n→σ*	Visible	R-band (German, radikalartig)
356.39	3.4789	0.0091	H→L-1 (90%)	n→σ*	Visible	
344.89	3.5948	0.0165	H→L-1 (87%)	n→σ*	Visible	
329.47	3.7632	0.0109	H+1→L-1 (83%)	n→σ*	Visible	
318.74	3.8899	0.0046	H→L-1 (92%)	n→π*	Visible	
312.91	3.9622	0.0010	H+1→L (89%)	n→π*	Visible	
Chloroform						
381.28	3.2518	0.0050	H→L (86%)	n→σ*	Visible	R-band (German, radikalartig)
373.53	3.3192	0.0121	H→L-1 (85%)	n→σ*	Visible	
365.04	3.3964	0.0079	H+1→L (78%)	n→σ*	Visible	
357.43	3.4687	0.0022	H+1→L-1(77%)	n→σ*	Visible	
353.08	3.5115	0.0038	H→L-1 (92%)	n→π*	Visible	
337.25	3.6763	0.0006	H+1→L (89%)	n→π*	Visible	
CCl_4						
421.64	2.9405	0.0070	H→L (86%)	n→σ*	Visible	R-band (German, radikalartig)
403.06	3.0760	0.0049	H→L-1 (85%)	n→σ*	Visible	
397.56	3.1165	0.0008	H+1→L (78%)	n→σ*	Visible	
390.56	3.1745	0.0037	H+1→L-1(74%)	n→σ*	Visible	
387.04	3.2034	0.0020	H→L-1 (92%)	n→π*	Visible	
375.68	3.3003	0.0013	H+1→L (89%)	n→π*	Visible	

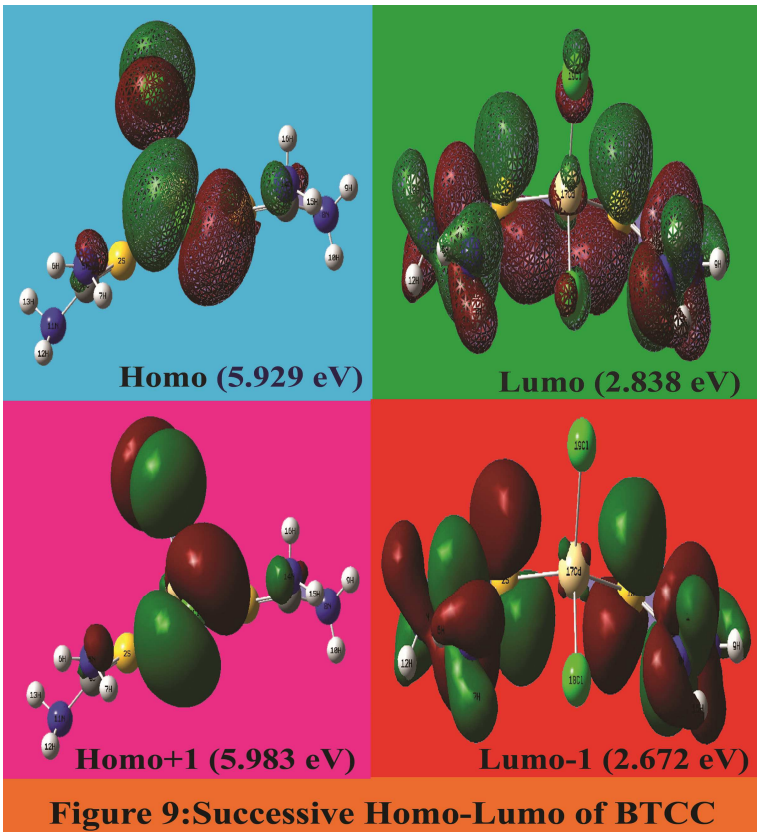

Figure 9:Successive Homo-Lumo of BTCC

TD-DFT calculations predict that, irrespective of the gas and solvent phase, the entire transitions belong to quartz

ultraviolet region. In the case of gas phase, the strong transitions are at 518.69, 505.48, 487.50, 474.04, 470.83 and 463.68 nm with an oscillator strength f = 0.0055, 0.0008, 0.0013, 0.0026, 0.0002 and 0.0035 with energy gap 2.3903, 2.4528, 2.5433, 2.6155, 2.6333 and 2.6739 eV. The transition is denoted by n→σ* belongs to visible region. The designation of the band is R-band (German, radikalartig) which is attributed to the above said transition of chain of chromophoric groups, such as Cadmium chloride group. They are characterized by low molar absorptivities (ξ_{max}<100) and undergo hypsochromic to bathochromic shift and the solvent effect is inactive in this compound. The simulated UV-Visible spectra in gas and solvent phase are shown in Figure 8.

In the case of DMSO solvent, strong transitions are 358.40, 356.39, 344.89, 329.47, 318.74 and 312.91 nm with an oscillator strength f=0.0125, 0.0091, 0.0165, 0.0109, 0.0046 and 0.0010 with maximum energy gap 3.9622 eV. They are assigned to n → π* transition and belongs to visible region. One of the electronic transitions is observed at IR region. This shows that, from gas to solvent, the electronic transitions retained at visible region. This view indicates that, the BTCC molecule has visible active and it is capable of having rich optical properties. In addition to that, the calculated optical band gap 3.9622 eV which also ensure that the present compound possessing LO as well as NLO properties. In view of calculated absorption spectra, the maximum absorption wavelength corresponds to the electronic transition from the HOMO+1 to LUMO-1 with maximum contribution. The Frontier molecular orbital diagram is presented in the Figure 9. In this present compound, the chromophores are Cadmium chloride group, the crystal properties are enhanced in the present compound.

Table 9: Calculated energies values, chemical hardness, electro negativity, Chemical potential, Electrophilicity index of Bis(thiourea) Cadmium Chloride (BTCC)

Parameters	TD-DFT/B3LYP/ 6-311G++(d, p)
E_{total} (Hartree)	-7449.82
E_{HOMO} (eV)	8.01
E_{LUMO} (eV)	0.83
$\Delta E_{HOMO\text{-}LUMO\ gap}$ (eV)	7.18
$E_{HOMO\text{-}1}$ (eV)	0.04
E_{LUMO+1} (eV)	0.18
$\Delta E_{HOMO\text{-}1\text{-}LUMO+1\ gap}$ (eV)	0.14
Chemical hardness (η)	3.59
Electronegativity (χ)	4.42
Chemical potential (μ)	3.59
Chemical softness(S)	0.1392
Electrophilicity index (ω)	2.0119
Dipole moment	3.8009

The chemical hardness and potential, electronegativity and Electrophilicity index are calculated and their values are shown in Table 9. The chemical hardness is a good indicator of the chemical stability. The chemical hardness of the present compound is 3.59 and therefore, the present compound has much chemical stability. The substitutions of Cd -C*l* group enhanced the chemical stability and metal character of the compound. Similarly, the electronegativity of the compound is 4.42; the property of chemical bond in the molecule will be changed from covalent to ionic. Accordingly, due to the addition of Cd, the bonds character of the compound rehabilitated to rich ionic. Electrophilicity index is a factor which is used to measure the energy lowering due to maximal electron flow between donor [HOMO] and acceptor [LUMO]. From the Table 9, it is found that the Electrophilicity index is 2.0119 which is high and this value ensures that the strong energy transformation is taking place between HOMO+1 and LUMO-1 instead of HOMO-LUMO since the transition is forbidden between HOMO and LUMO. The dipole moment in a molecule is another important electronic property. Whenever the molecule would have possessing large dipole moment, the intermolecular interactions are very strong. The calculated dipole moment value for the title compound is 3.8009 Debye. It is apparent and moderate due to the presence of coordinate covalent bond which is inferred that, the present molecule has strong intermolecular interactions.

Molecular electrostatic potential (MEP) maps studies

The molecular electrostatic potential surfaces illustrate the charge distributions of molecules three dimensionally. This map allows us to visualize variably charged regions of a molecule. Knowledge of the charge distributions is much useful to determine how molecules interact with protein and it is also be used to determine the requirement of minimum energy to bind with protein structure [52]. Molecular electrostatic potential view is mapped up at the level of B3LYP/3-21G (d, p) theory with optimized geometry. There is a great deal of intermediary potential energy, the non red or blue region indicate that the electro negativity difference is not very great. In a molecule with a great electro negativity difference, charge is very polarized in negative and positive form, and there are significant differences in electron density in different regions of the molecule. This great electro negativity difference leads to regions that are almost entirely red and almost entirely blue. The region of intermediary potential is explored by

yellow and green color and the regions of extreme potential look at red and blue colors are key indicators of electronegativity.

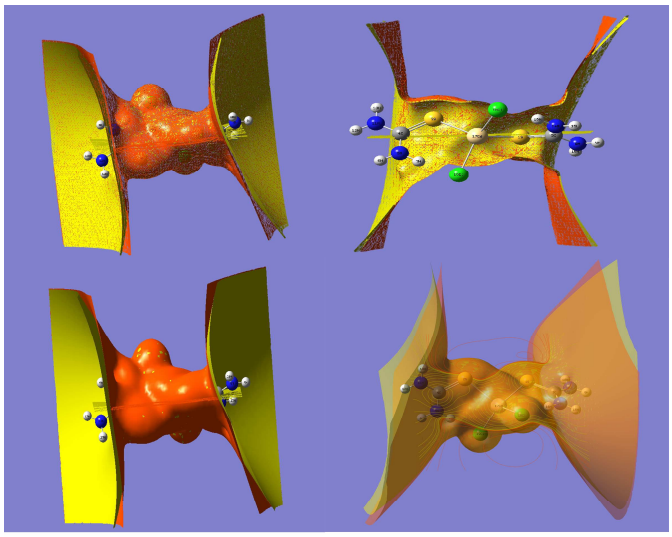

Figure 10: MEP map diagram with isosurface of BTCC

The color code of these maps is in the range between -7.86 a.u. (deepest red) to 7.86 a.u. (deepest blue) in compound. The positive (blue) regions of MEP are related to electrophilic reactivity and the negative (green) regions to nucleophilic reactivity shown in Figure 10. As can be seen from the MEP map of the title molecule, the negative regions are mainly localized on Cadmium chloride and sulphur atoms. A maximum positive region is localized on the H of NH_2 groups indicating a possible site for nucleophilic attack. Though, this molecule contains different electron rich atoms, the negative potential regions located at metal combined atoms. From these results, it is found that, the metal atoms coupled strongly in the inertial position of organic lattice site.

Polarizability and First order hyperpolarizability calculations

In order to investigate the relationships among the molecular structures, non-linear optic properties (NLO) and molecular binding properties, the polarizabilities and first order hyperpolarizabilities of the present compound are calculated using DFT-B3LYP method and 3-21 G (d, p) basis set, based on the finite-field approach.

The Polarizability and hyperpolarizability tensors (α_{xx}, α_{xy}, α_{yy}, α_{xz}, α_{yz}, α_{zz} and β_{xxx}, β_{xxy}, β_{xyy}, β_{yyy}, β_{xxz}, β_{xyz}, β_{yyz}, β_{xzz}, β_{yzz}, β_{zzz}) are obtained from the output file of Polarizability and hyperpolarizability calculations. However, α and β values of Gaussian output in atomic units (a.u.) have been converted into electronic units (esu) (α; 1 a.u. = 0.1482×10^{-24} esu, β; 1 a.u. = 8.6393×10^{-33} esu). The mean polarizability (α), anisotropy of polarizability ($\Delta\alpha$) and the average value of the first hyperpolarizability $\langle\beta\rangle$ can be calculated using the equations.

$$\alpha_{tot} = \frac{1}{3}\left(\alpha_{xx} + \alpha_{yy} + \alpha_{zz}\right)$$

$$\Delta\alpha = \frac{1}{\sqrt{2}}\left[\left(\alpha_{xx} - \alpha_{yy}\right)^2 + \left(\alpha_{yy} - \alpha_{zz}\right)^2 + \left(\alpha_{zz} - \alpha_{xx}\right)^2 + 6\alpha_{xz}^2 + 6\alpha_{xy}^2 + 6\alpha_{yz}^2\right]^{\frac{1}{2}}$$

$$\langle\beta\rangle = \left[\left(\beta_{xxx} + \beta_{xyy} + \beta_{xzz}\right)^2 + \left(\beta_{yyy} + \beta_{yzz} + \beta_{yxx}\right)^2 + \left(\beta_{zzz} + \beta_{zxx} + \beta_{zyy}\right)^2\right]^{\frac{1}{2}}$$

It is well known that, molecule with high values of dipole moment, molecular Polarizability and first hyperpolarizability having more active NLO properties. The first hyperpolarizability (β) and the component of hyperpolarizability β_x, β_y and β_z of BTCC along with related properties (μ_0, α_{total}, and $\Delta\alpha$) are reported in Table 10. The calculated value of dipole moment is found to be 2.3036 Debye. The highest value of dipole moment is observed in the component of μ_y which is 2.3028 Debye. The lowest value of the dipole moment of the compound is μ_x component (-0.0629 D). The calculated average Polarizability and anisotropy of the Polarizability are $171.274\text{x}10^{-24}$ esu and $209.966\text{x}10^{-24}$ esu, respectively. The high value of Polarizability reflects the rich NLO property of the present compound. The magnitude of the molecular hyperpolarizability β, is one of the important key factors in NLO system. The B3LYP/3-21 G (d, p) calculated first hyperpolarizability value (β) is $1304.70\text{x}10^{-30}$ esu. The hyperpolarizability result explore that, the title compound is able to generate the second order harmonic

generation with more amplitude. So, the present compound can be used to prepare the NLO crystals for electronic applications. In addition to that, due to its elevated values of Polarizability and hyperpolarizability, the present compound is able to bind with other molecules with less amount of binding energy.

Table 10: The dipole moments μ (D), the polarizability α (a.u.), the average polarizability α_o (esu), the anisotropy of the polarizability Δα (esu), and the first hyperpolarizability β (esu) of Bis(thiourea) Cadmium Chloride (BTCC)

Parameter	a.u.	Parameter	a.u.
α_{xx}	-23.5120	β_{xxx}	-1.6716
α_{xy}	0.0191	β_{xxy}	7.3234
α_{yy}	-125.9574	β_{xyy}	-0.2801
α_{xz}	-0.0786	β_{yyy}	-11.8204
α_{yz}	12.6020	β_{xxz}	58.2961
α_{zz}	-127.7143	β_{xyz}	0.2798
α_{tot}	171.274	β_{yyz}	-14.0302
Δα	209.966	β_{xzz}	-0.2119
μ_x	-0.0629	β_{yzz}	14.8567
μ_y	2.3028	β_{zzz}	5.8425
μ_z	-0.0116	β_{tot}	1304.70
μ	2.3036		

Second Harmonic Generation (SHG) Studies

The second harmonic generation test was carried out by classical powder method developed by Kurtz and Perry. It is an important and popular tool to evaluate the conversion efficiency of NLO materials. The fundamental beam of 1064 nm from Q switched Nd: YAG laser was used to test the second harmonic generation (SHG) property of pure BTCC crystals. Pulse energy 2.9 mJ/pulse and pulse width 8 ns with a repetition rate of 10 Hz were used. The photo multiplier tube (Hamahatsu R2059) was used as detector and 90 degree geometry was employed. The input laser beam was passed through an IR detector and then directed on the microcrystalline powdered sample packed in a capillary tube. The SHG signal generated in the sample was confirmed from the emission of green light from the sample [53]. The SHG output of pure BTCC crystal was 98 mV. The SHG output confirms the nonlinear nature of the experimental crystal.

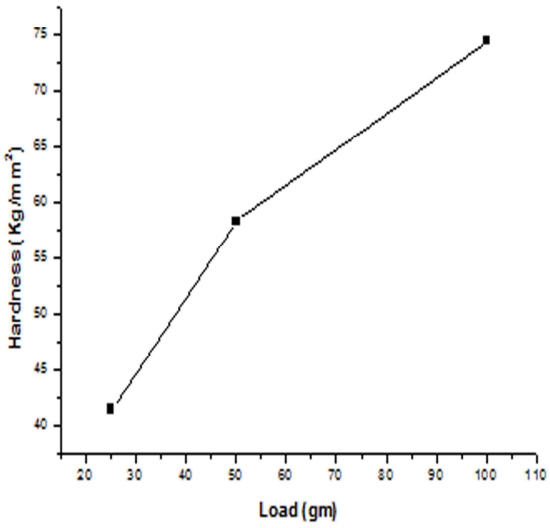

Figure 11: Variation of Hardness with Load of BTCC Crystals

Micro Hardness Studies

Vicker's micro hardness test was carried out for pure BTCC crystals. Among the several of hardness measurement, the most common and reliable method is the Vicker's hardness test method. In this method, micro indentation is made on the surface with the help of a diamond pyramidal indenter. Hardness is generally defined as the ratio of the load applied to the surface of the indentation. The Vicker's hardness against load is drawn for BTCC crystals in Figure 11. Vicker's microhardness test conducted on the experimental crystal proves its greater physical strength. It is well explained by the increase in hardness value with increase in Load and shown in Table 11.

Table 11: Microhardness of BTCC crystals

S. No.	Load (grams)	BTCC (HV)
1	25	41.4
2	50	58.2
3	100	74.4

Thermodynamical functions analysis

Normally, the thermo dynamical analysis on aromatic compound is important since they provide the necessary information regarding the chemical reactivity. In addition to that, it is also very important to discuss the existence and alternation of thermodynamic parameters of the present compound since it is a metallo-organic substance. On the basis of vibrational analysis at B3LYP/3-21 G (d, p) level, the standard statistical thermodynamic functions: standard heat capacities ($C^0_{p,m}$), standard entropies (S^0_m) and standard enthalpy changes ($\Delta H^0 m$) for the title compound were obtained from the theoretical harmonic frequencies and listed in Table 12. From the table 12, it can be observed that, the thermodynamic functions were increased with temperature ranging from 100 to 1000 K due to the fact that the molecular vibrational intensities increased with temperature. The correlation graph between heat capacities, entropies, enthalpy changes and temperatures were shown in Figure 12. At low temperature, it is found that, the specific heat capacity of the present compound is fall down rapidly and obeyed the Debye T^3 law whereas, at high temperature, the specific heat capacity is saturated at 1000 K. The entropy and enthalpy of the present compound gets elevated and saturated at 1000 K as the specific heat capacity.

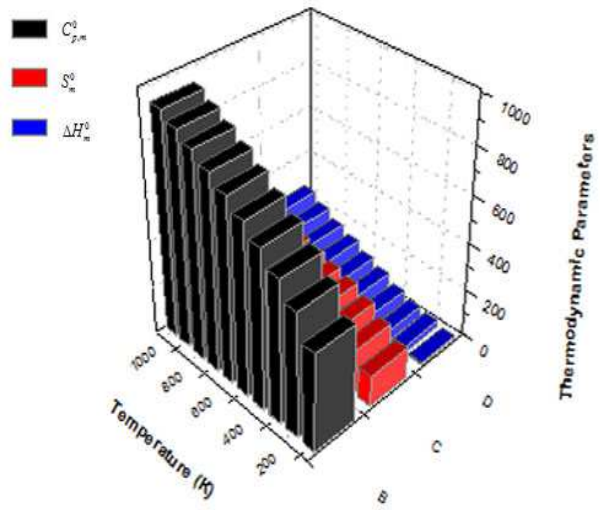

Figure 12: Thermodynamical Parameters at different temperatures of BTCC

Table 12: Thermodynamic parameters at different temperatures at the B3LYP/3-21G (d, p) level for Bis(thiourea) Cadmium Chloride (BTCC)

T(K)	$C^0_{p,m}$ (cal mol^{-1} K^{-1})	S^0_m (cal mol^{-1} K^{-1})	ΔH^0_m (kcal mol^{-1})
100.00	403.79	130.51	9.05
200.00	509.83	179.76	24.63
298.15	589.42	220.15	44.33
300.00	590.78	220.83	44.73
400.00	658.98	253.66	68.52
500.00	718.52	279.92	95.25
600.00	771.49	301.07	124.33
700.00	819.24	318.35	155.33
800.00	862.72	332.81	187.91
900.00	902.65	345.18	221.82
1000.00	939.59	355.95	256.89

CONCLUSION

In the present investigation, complete vibrational analysis of BTCC has been done using experimental and computational methods. The chronological change of finger print and group frequency region of the organic part with respect to the functional group (metal chloride) has also been monitored. The BTCC crystals were characterized by single crystal XRD, powder XRD, FTIR, FT-Raman, UV-Vis-NIR analysis, second harmonic generation and Vicker's micro hardness studies. The lattice parameters obtained from single crystal XRD matches with that of lattice parameters were calculated from powder XRD. The presence of functional groups and the coordination of metal ions to thiourea through sulphur were confirmed by FTIR and FT-Raman analysis. The UV-Vis-NIR analysis reveals that the BTCC crystals are having good transparency in the entire visible region. The nonlinear optical (NLO) efficiency of the BTCC crystals was determined by the second harmonic generation studies. The results of Vicker's micro hardness studies reveal that all the experimental crystals have greater physical strength. The change of geometrical parameters along with the substitutions is deeply analyzed. The simulated ^{13}C NMR and ^{1}H NMR spectra in gas and solvent phase are displayed and the chemical shifts related to TMS are studied. The electrical and optical and bio molecular properties are profoundly investigated using frontier molecular orbital. From the UV-Visible spectra, it is monitored that, the entire electronic transitions shifted bathochromically due to the substitutional effect. It is also found that the present compound is optically and electrically active and also posses NLO properties. The molecular electrostatic potential (MEP) map is performed and from which the change of the chemical properties of the compound is also discussed.

REFERENCES

[1]V Venkataramanan; S Maheswaran; JN Sherwood; HL Bhat, *Journal of Crystal Growth*, **1997**, 179, 605-610.
[2]S Chenthamarai; D Jayaraman; C Subramanian; P Ramasamy, *Materials Letters*, **2001**, 47, 247-251.
[3]K Ambujam; K Rajarajan; S Selvakumar; A Joseph; P Sagayaraj, *Journal of Crystal Growth*, **2006**, 286, 440-444.
[4]SS Hussaini; NR Dhumane; G Rabbani; P Karmuse; VG Dongre; MD Shirsat, *Crystal Research and Technology*, **2007**, 42, 1110-1116.
[5]SS Hussaini; NR Dhumane; VG Dongre; P Karmuse; P Ghughare; MD Shirsat, *Optoelectronics and Advanced Materials-Rapid Communications*, **2008**, 2, 108-112.
[6]V Kannan; NP Rajesh; R Bairava Ganesh; P Ramasamy, *Journal of Crystal Growth*, **2004**, 269, 565- 569.
[7]K Meera; R Muralidharan; R Dhanasekaran; P Manyum; P Ramasamy, *Journal of Crystal Growth*, **2004**, 263, 510-516.
[8]MH Jiang; Q Fang, *Advanced Materials*, **1999**, 11, 1147-1151.
[9]J Ramajothi; S Dhanushkodi; K Nagarajan, *Crystal Research and Technology*, **2004**, 39, 414-420.
[10]S Ariponnammal; S Radhika; R Selva; N Victor Jeya, *Crystal Research and Technology*, **2005**, 40, 786-788.
[11]MJ Rosker; P Cunningham; MD Ewbank; HO Marcy; FR Vachss; LF Warren; R Gappinger; R Borwick, *Pure and Applied Optics*, **1996**, 5, 667.
[12]K Selvaraju; R Valluvan; K Kirubavathi; S Kuma- raraman, *Optics Communications*, **2007**, 269, 230- 234.
[13]KH Hellwege; AM Hellwege; Landolt–Bornstein, Numerical Data and Functional Relationships in Science and Technology Group II, Springer, Berlin, **1982**.
[14]SG Bhat; SM Dharmaprakah, *Mater. Res. Bull.*, **1998**, 33, 833.
[15]N Karthick; RSankar; RJayavel; SPandi, *Journal of Crystal Growth*, **2009**, 312, 114.
[16]S Anie Roshan; Cyriac Joseph; MA Ittyachen, *Mater. Lett*., **2001**, 49.
[17]G SenthilMurugan; P Ramasamy, *Journal of Crystal Growth*, **2009**, 311, 585.
[18] M Lydia Caroline; S Vasudevan, *Mater. Chem. Phys*., **2009**, 113, 670.
[19]G Senthil Murugan; N Balamurugan; P Ramasamy, *Mater. Lett*., **2008**, 62, 3087.
[20]R S Sundararajan; M Senthilkumar; C Ramachandraraja, *Journal of Minerals and Materials Characterization and Engineering*, **2013**, 1, 315-320.
[21]RJ Lewis; Sr (Ed), Hawley's Condensed Chemical Dictionary, 12th edition New York, NY, Van Nostrand Rheinhold Co, **1993**, 860.
[22]D Hartley; H Kidd (eds), The Agrochemicals Handbook Old Working, Surrey, United Kingdom, Royal Society of Chemistry, Unwin Brothers Ltd., **1983**.
[23]W Gerhartz, Ullmann's Encyclopedia of Industrial Chemistry 5th edition, Deerfield Beach, FL: VCH Publishers, **1985**, 21.
[24]MK Marchewka; A Pietraszko, *Spectrochimica Acta PartA*, **2008**, 69, 312–318.
[25]Ivan S Lim; Gustavo E Scuseria, *Chemical Physics Letters*, **2008**, 460, 137-140.
[26]Ljupco Pejov; Mirjana Ristova; Bojan Soptrajanov, *Spectrochimica Acta PartA*, **2011**, 79, 27–34.
[27]MJ Frisch et al, Gaussian 09, Revision A1, Gaussian, Inc. Wallingford CT., **2009**.
[28]Z Zhengyu; D Dongmei, *Journal of Molecular Structure*, **2000**, 505, 247-252.

[29]Z Zhengyu; F Aiping; D Dongmei, *Journal of Quantum Chemistry*, **2000**, 78, 186-189.
[30]AD Becke, *Physics Review*, **1988**, A38, 3098-3101.
[31]C Lee; W Yang; RG Parr, *Physics Review*, **1988**, B37, 785-790.
[32]AD Becke, *Journal of Chemical Physics*, **1993**, 98, 5648-5652.
[33]LJ Bellamy, The Infrared Spectra of Complex Molecules, Chapman and Hall, London, **1980**, 2.
[34]Mehmet Karabacak; Emel Postalcilar; Mehmet Cinar, *Spectrochimica Acta PartA*, **2012**, 85, 261– 270.
[35]RM Silverstein; FX Webster, Spectrometric Identification of Organic Compounds, 6th edition, Wiley, New York, **1998**.
[36]S Pandiarajan; M Umadevi; RK Rajaram; V Ramakrishnan, *Spectrochimica Acta PartA*, **2005**, 62, 630-636.
[37]JR During; MM Bergana; HV Phan, *Journal of Raman Spectroscopy*, **1991**, 22,141.
[38]G Varsanyi, Vibrational spectra of benzene derivatives, Academic press, New York, **1969**.
[39]N Vijayan; RR Babu; R Gopalakrishnan; P Ramasamy; M Ichimura; M Palanichamy, *Journal of Crystal Growth*, **2005**, 564–569.
[40]R Shanmugam; D Sathayanarayana, *Spectrochimica Acta PartA*, **1984**, 40.
[41]M Silverstein; GC Basseler; C Morill, spectrochemtric identification of organic compound, wiley, New York, **1981**.
[42]LJ Bellamy; RL Williams, *Spectrochimica Acta*, **1957**, 341.
[43]V Arjunan; S Mohan, *Spectrochimica Acta partA*, **2009**, 72, 436-444.
[44]J Swaminathan; MRamalingam; N Sundaraganesan, *Spectrochimica Acta PartA*, **2009**, 71, 1776 – 1782.
[45]K Nakamoto, Infrared and Raman Spectra of Inorganic and Coordination Compounds, 5th edition, Wiley, New York, **1997**.
[46]S D Ross, Inorganic Infrared and Raman Spectra, McGraw- Hill, London, **1972**.
[47]Vibrational Spectra of Some Coordinated Ligands Spectrosc. Prop. Inorganic. Organomet. Compounds, **1968**, I.
[48]Characteristic Vibrations of Compounds of Main Group Elements I to VIII, Spectrosc. Prop. Inorganic Organomet. Compounds, **1968**, I.
[49]G Socrates, Infrared and Raman characteristics group frequencies third edition, Wiley, New York, **2001**.
[50]Jean; Yvesand; Volatron, François An Introduction to Molecular Orbital's Oxford University Press, **2005**, 1103.
[51]SI Gorelsky, SWizard Program Revision45, University of Ottawa, Ottawa, Canada, **2010**.
[52]S Ramalingam; S Periandy; S Sugunakala; T Prabhu; M Bououdina, *Spectrochimica Acta PartA*, **2013**, 115, 118–135.
[53]S K Kurtz; T T Perry, *Journal of Applied Physics*, **1968**, 39, 3798.